



Isopropanol decomposition on carbon based acid and basic catalysts

J. Bedia, J.M. Rosas, D. Vera, J. Rodríguez-Mirasol, T. Cordero*

Chemical Engineering Department, School of Industrial Engineering, University of Málaga, Campus de Teatinos s/n, 29071 Málaga, Spain

ARTICLE INFO

Keywords:

Isopropanol
Dehydration
Dehydrogenation
Carbon catalyst

ABSTRACT

Chemical activation of biomass waste with different activating agents allows the preparation of activated carbons with a relatively highly porous development and different surface chemistry properties. Acidic and basic carbon based catalysts have been prepared by chemical activation of olive stone waste with H_3PO_4 and H_2SO_4 of acid character and $\text{Ca}(\text{OH})_2$ and $\text{Ba}(\text{OH})_2$ of basic character. The carbons have been tested as catalysts for the isopropanol decomposition reaction. The acidic carbons show higher steady state conversions than those corresponding to the basic carbons. The highest conversions were obtained using the carbon activated with phosphoric acid as catalyst. In the absence of oxygen acidic carbon based catalysts dehydrate isopropanol to propylene. In the case of the basic carbon catalysts, the carbon activated with $\text{Ba}(\text{OH})_2$ mainly dehydrogenates isopropanol to acetone, with low production of propylene. The carbon activated with $\text{Ca}(\text{OH})_2$ presents acid and basic surface sites and propylene and acetone are obtained on this catalyst. In the presence of oxygen, the acidic carbons show higher conversion values and part of the isopropanol suffers oxidative dehydrogenation yielding acetone as well as propylene, although at high isopropanol steady state conversion values only propylene is obtained.

© 2010 Elsevier B.V. All rights reserved.

1. Introduction

Flash pyrolysis of biomass produces liquid oil (bio-oil) constituted mostly by oxygenated compounds, which are of great interest as fuel [1,2]. Like the biomass precursor, this bio-oil contains almost negligible amount of nitrogen, sulfur and metals. However, transformation of bio-oil is necessary to reach a quality similar to that of the conventional fuel. Studies have been conducted to improve the quality of bio-oil as fuel through catalytic processes with inorganic acid solids [3–5]. Gayubo et al. [4] studied the catalytic transformation of several model components of biomass pyrolysis oil, such as phenols and alcohols (1-propanol, isopropanol, 1 and 2-butanol, etc), over HZSM-5 zeolite obtaining mainly light olefins and aromatics.

Nowadays, nearly 90% of acetone is coproduced with phenol by the cumene route. This technique is the preferred technology because of its lower cost. The main process for manufacturing cumene involves the reaction of propylene and benzene in the presence of phosphoric acid-based catalysts or, more recently, zeolite catalysts. The cumene is oxidized in the liquid phase to cumene hydroperoxide, which is then cleaved in the presence of sulfuric acid to phenol and acetone. About 0.62 tons of acetone is produced per ton of phenol obtained. The production of acetone from only cumene would require a balancing of the market with the

coproduct phenol from this process. Therefore, there is a need for alternative acetone production routes. In the isopropyl alcohol route, the alcohol is dehydrogenated to acetone over a metal, metal oxide or salt catalyst. Acetone could be obtained from isopropanol alcohol by either dehydrogenation or air oxidation.

Propylene is a key building block for the petrochemical industry used for the production of polypropylene, acrylonitrile, propylene oxide, cumene, oxo-alcohols and other intermediates. Propylene demand has grown from 16.4 million tons in 1980 to 69.0 million tons in 2006 and the demand is expected to increase faster than supply up to 350 million tons in 2020 [6]. Nowadays propylene is obtained from non-renewable sources mainly as by-product of ethylene production in stream crackers and from refinery in FCC streams. Therefore, the finding and developing of new processes for propylene production from renewable sources is of great interest from economical and environmental point of views.

Activated carbons are mainly used as adsorbents and catalyst supports. However, the special characteristics of these materials related to their porous structure and surface chemistry make them suitable to be used also as catalysts per se [7]. Activated carbons show some important advantages to be used as catalysts [8], such as high specific surface area, high thermal and chemical stability and the possibility to be obtained from many diverse materials including different types of lignocellulosic waste [9–15]. Carbon materials can be used as catalysts for acid/base reactions due to the presence of surface oxygen groups of acidic and/or basic character [16,17].

Alcohol decomposition is also used as test reaction for the evaluation of the acid–base properties of catalysts. Alcohol dehy-

* Corresponding author. Tel.: +34 952132038; fax: +34 952132038.
E-mail address: cordero@uma.es (T. Cordero).

Nomenclature

$A_{\text{BET}}^{\text{N}_2}$	apparent surface area (m^2/g)
$A_{\text{t}}^{\text{N}_2}$	external surface area (m^2/g)
E_a	apparent activation energy (kJ/mol)
F_{olIPA}	isopropanol molar flow rate (mol s^{-1})
FTIR	Fourier transform infrared spectroscopy
IPA	isopropanol
k	apparent rate constant ($\text{mol atm}^{-1} \text{g}^{-1} \text{s}^{-1}$)
k_o	preexponential factor ($\text{mol atm}^{-1} \text{g}^{-1} \text{s}^{-1}$)
P/P_o	nitrogen relative pressure
P_{olIPA}	isopropanol inlet partial pressure (atm)
Py	pyridine
r	isopropanol reaction rate ($\text{mol IPA s}^{-1} \text{g}^{-1}$)
R	impregnation ratio (weight of activating agent relative to that of dry precursor)
Sa	Selectivity to acetone
Sp	Selectivity to propylene
STP	standard temperature pressure conditions
T	temperature (K)
TPD	temperature-programmed desorption
V_{ads}	nitrogen volume adsorbed ($\text{cm}^3 \text{STP g}^{-1}$)
$V_{\text{t}}^{\text{N}_2}$	micropore volume ($\text{cm}^3 \text{g}^{-1}$)
W	catalyst weight (g)
W/F_{olIPA}	isopropanol space-time (g s mol^{-1})
X	isopropanol conversion
XPS	X-ray photoelectron spectroscopy

drogenation products (aldehydes and ketones) are preferentially formed on basic catalysts, while dehydration products (olefins and ethers) are favored when acidic sites are present [18]. It is generally accepted that isopropanol decomposition over basic sites proceeds through an elimination reaction yielding acetone. Over acid sites, isopropanol dehydrates to propylene and to di-isopropyl ether [19]. In this study, home-made acid and basic carbons were studied as catalysts for the selective catalytic decomposition of isopropanol (as model compound of bio-oil). Activated carbons with surface acidity were obtained by chemical activation of a biomass material with H_3PO_4 and H_2SO_4 . Activated carbons with surface basicity were obtained by chemical activation of a biomass material with $\text{Ca}(\text{OH})_2$ and $\text{Ba}(\text{OH})_2$. The effect of the presence of oxygen in the isopropanol decomposition was also analyzed.

2. Experimental

2.1. Catalysts synthesis methods

The carbon catalysts were obtained from olive stone waste. The raw olive stone waste shows a negligible porous structure. The olive stone was impregnated at room temperature with the different activating agents, namely, H_3PO_4 (85 wt.% in H_2O , Aldrich), H_2SO_4 (95.0–98.0%, Sigma–Aldrich), $\text{Ca}(\text{OH})_2$ ($\geq 95\%$, Sigma–Aldrich) and $\text{Ba}(\text{OH})_2$ ($\sim 95\%$, Aldrich), at different impregnation ratios (R = weight of activating agent relative to that of dry precursor). The impregnated samples were activated under continuous N_2 flow ($150 \text{ cm}^3 \text{STP}/\text{min}$), in a conventional tubular furnace at different temperatures. These temperatures were reached at a heating rate of $10^\circ\text{C}/\text{min}$ and maintained for 2 h. The activated samples were cooled inside the furnace, maintaining the N_2 flow and then washed with distilled water at 60°C . The resulting carbon catalysts were dried at 100°C . Table 1 reports the notation and activation conditions (impregnation ratio and carbonization temperature) of the different carbons obtained. The nomenclature used for the carbon based catalysts was PAC, SAC, BaAC and CaC

Table 1

Notation and activation conditions (impregnation ratio and carbonization temperature) for the different carbons obtained.

Carbon catalyst	Impregnation ratio	Activating agent	Activation temperature ($^\circ\text{C}$)
PAC-550	1	H_3PO_4	550
SAC-600	1	H_2SO_4	600
SAC-900	1	H_2SO_4	900
CaAC-900	3	$\text{Ca}(\text{OH})_2$	900
BaAC-700	3	$\text{Ba}(\text{OH})_2$	700

when H_3PO_4 , H_2SO_4 , $\text{Ba}(\text{OH})_2$ and $\text{Ca}(\text{OH})_2$ were used as activating agents, respectively, followed by the activation temperature in degrees Celsius.

2.2. Catalyst characterization

The porous structure of the carbons was characterized by N_2 adsorption–desorption at -196°C , carried out in a 2020 ASAP model of Micromeritics. Samples were previously outgassed during at least 8 h at 150°C . From the N_2 adsorption/desorption isotherm, the apparent surface area ($A_{\text{BET}}^{\text{N}_2}$) was determined applying the BET equation [20], the micropore volume ($V_{\text{t}}^{\text{N}_2}$) and the external surface area ($A_{\text{t}}^{\text{N}_2}$) were calculated using the t -method [21].

The surface chemistry of the samples was analyzed by temperature-programmed desorption (TPD), X-ray photoelectron spectroscopy (XPS) and Fourier transform infrared spectroscopy (FTIR). TPD profiles were obtained in a custom quartz tubular reactor placed inside an electrical furnace. The samples were heated from room temperature up to 900°C at a heating rate of $10^\circ\text{C}/\text{min}$ in a helium flow ($200 \text{ cm}^3 \text{STP}/\text{min}$). The amounts of CO and CO_2 desorbed from the samples were monitored with non-dispersive infrared (NDIR) gas analyzers (Siemens ULTRAMAT 22). X-ray photoelectron spectroscopy (XPS) analyses of the samples were obtained using a 5700C model Physical Electronics apparatus, with $\text{MgK}\alpha$ radiation (1253.6 eV). For the analysis of the XPS peaks, the C1s peak position was set at 284.5 eV and used as reference to position the other peaks. Infrared (FTIR) spectra were obtained using a Bruker Optics Tensor 27 FTIR spectrometer by adding 256 scans in the $4000\text{--}400 \text{ cm}^{-1}$ spectral range at 4 cm^{-1} resolution. Pressed KBr pellets at a sample/KBr ratio of around 1:250 were used.

The type of surface acidity (Brønsted or Lewis) was studied by FTIR of the carbons with pyridine (Py) chemisorbed at 100°C . The inlet partial pressure of the organic base was 0.02 atm and it was established saturating He with pyridine in a saturator at controlled temperature. After saturation of the carbon, desorption is carried out at the adsorption temperature in helium flow.

2.3. Isopropanol dehydration

The activities of the catalysts were measured by the decomposition of isopropanol (IPA) performed at atmospheric pressures, in a quartz fixed bed microreactor (4 mm i.d.) placed inside a vertical furnace with temperature controlled, using 100 mg of catalyst ($100\text{--}300 \mu\text{m}$ particle size) dispersed in quartz. Nitrogen or air was saturated with isopropanol (Sigma–Aldrich, 99.5%, HPLC grade) vapor by contact in a saturator at 10°C resulting in a partial pressure of 0.0185 atm . To avoid the condensation of isopropanol or any reaction product, all the lines from the saturator to the chromatograph were heated above 120°C . The gas reaction mixture feeds the reactor at $100 \text{ cm}^3 \text{STP}/\text{min}$, corresponding to a space-time of $W/F_{\text{olIPA}} = 0.073 \text{ g s } \mu\text{mol}^{-1}$. Reactant and products concentrations were measured by gas chromatography (Perkin-Elmer Autosystem GC with a 50 m HP-1 methyl silicone capillary column and flame ionization detector).

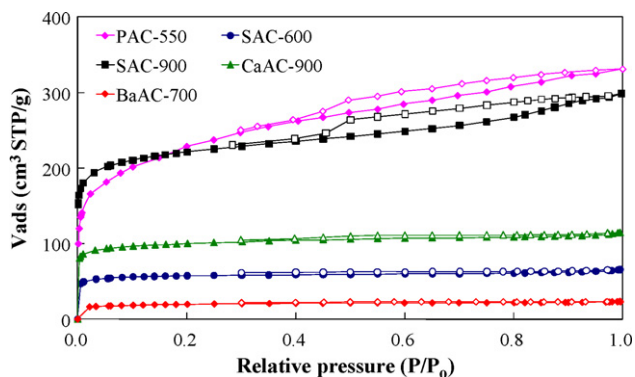


Fig. 1. N₂ adsorption–desorption isotherms at –196 °C of the carbon catalysts (adsorption: closed symbols; desorption: open symbols).

The reaction rate, r , was defined as the mol number of isopropanol transformed in one second per gram of catalyst. The conversion was defined as the ratio of the amount of isopropanol converted to the amount of isopropanol supplied to the reactor. The selectivity (in mol%) was defined as the molar ratio of a specific hydrocarbon product to all the hydrocarbons products formed. The carbon balance was reached with an error lower than 3%.

3. Results and discussion

Fig. 1 presents the N₂ adsorption–desorption isotherms at –196 °C of the different carbon catalysts. Carbons SAC-600, CaAC-900 and BaAC-700 show type I isotherms characteristic of solids with to a predominantly microporous structure. The isotherms of these carbons have an almost negligible hysteresis cycle which indicates the lack of a developed mesoporosity. The increase of the activation temperature from 600 to 900 °C when using sulfuric acid as activating agent results in a carbon which adsorbs much more nitrogen as a consequence of a more developed porous structure. Carbon SAC-900 shows a modified type I isotherms with a slight increase of the N₂ adsorbed with the relative pressures and a well developed H4 hysteresis cycle, associated to type I isotherms, which closes at a relative pressure value of 0.4, indicative of capillary condensation in mesopores. This isotherm is characteristic of an essentially microporous solid with a slightly developed mesoporosity. Finally, the carbon prepared by activation with H₃PO₄, PAC-550, shows an isotherm with an open knee, which extends up to increasingly higher relative pressures characteristic of wide microporosity. It is noticeable the presence of the hysteresis cycle up to high relative pressures. The isotherm is characteristic of a well-developed microporous structure with a significant contribution of mesoporosity. During the activation process, phosphoric acid is combined with organic species to form phosphate and polyphosphate bridges that separate and expand the organic structure. After removal of the acid, the carbon matrix results in an expanded state with an accessible pore structure [17,22].

Table 2 summarizes the structural parameters obtained from the N₂ adsorption–desorption isotherms. The carbons show apparent

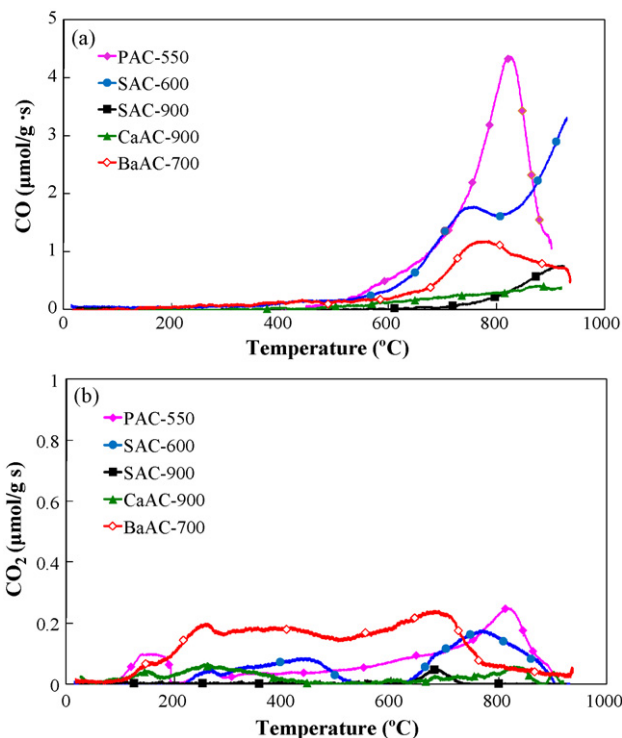


Fig. 2. TPD spectra for different carbons: (a) CO evolution; (b) CO₂ evolution.

surface areas between 68 m²/g for that obtained by activation with Ba(OH)₂ to 830 m²/g for that prepared by activation with H₃PO₄ at a activation temperature of 550 °C. Most of the carbons, except for PAC-550 and SAC-900, show low external surface areas, $A_t^{N_2}$, indicative of their predominantly microporous structure. PAC-550 and SAC-900 carbons display higher values of external surface area and micropore volumes, $V_t^{N_2}$, as a consequence of their more developed porous structure.

TPD analysis was used to characterize the different oxygen surface groups of the activated carbons, whose nature and amount depend on the starting material and the activation treatment [23]. Carbon–oxygen groups of acidic character (carboxylic, lactonic) evolve as CO₂ upon thermal desorption, whereas the non-acidic (carbonyl, ether, and quinone) and phenol groups give rise to CO. Anhydride surface groups evolve as both CO and CO₂. **Fig. 2a** and **b** depict the CO and CO₂ profiles, respectively, obtained from TPD experiments. All the carbons desorb most of the CO at high temperatures ($T > 700$ °C). The carbon PAC-550 desorbs a high amount of CO. It is reported that phosphoric acid activation generates a significant amount of groups of high thermal stability, which desorb as CO in the TPD experiments at high temperatures [16,24]. A lower amount of CO is desorbed at lower temperatures ($T < 700$ °C) as a consequence of decomposition of anhydride, phenol and ether groups. Carbons SAC-900 and CaAC-900 show the lowest amount of CO desorbed as a consequence of the high carbonization temperature used in their preparation.

Table 2

Porous structural parameters, obtained from N₂ isotherms, and amount of CO and CO₂ evolved from TPD analyses.

Carbon catalyst	N ₂ isotherm			TPD	
	$A_{BET}^{N_2}$ (m ² /g)	$A_t^{N_2}$ (m ² /g)	$V_t^{N_2}$ (cm ³ /g)	CO (μmol/g)	CO ₂ (μmol/g)
PAC-550	830	130	0.318	4070	270
SAC-600	194	10	0.085	3520	220
SAC-900	754	112	0.301	500	20
CaAC-900	338	24	0.150	610	110
BaAC-700	68	5	0.029	2180	410

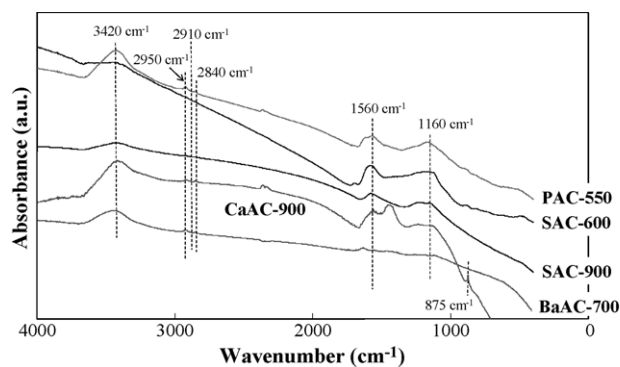


Fig. 3. FTIR spectra of the carbon catalysts.

CO₂ profiles show lower desorbed amounts compared to those for CO, indicating a lower presence of carboxyl, lactonic and anhydride groups on the surface of the different carbon catalysts. For the catalysts PAC-550 and SAC-600, it is noteworthy the evolution of CO₂ at around 800 °C that seems to be related to the evolution of CO at this temperature [24]. Evolution of CO₂ at this high temperature may be due to secondary reactions between CO and oxygen surface complexes [25].

The amount of CO and CO₂ evolved during the TPD experiments obtained by the integration of the areas under the TPD curves is summarized in Table 2. As previously mentioned, the amount of CO evolved is higher than that of CO₂. The high amount of CO₂ evolved during the TPD of the Ba containing sample may probably be connected with carbonates formation on this sample during drying in air. Additionally, some oxygen surface groups of acidic character (carboxylic and lactones) may be formed during the activation process that would evolve as CO₂ in the TPD. Decomposition of carbonate formed during the activation step may be responsible for the CO₂ evolution at about 700 °C. The literature shows examples of decomposition of the alkaline metal carbonates at temperatures below the melting point when heating carbonate–carbon mixtures [26]. The highest amount of oxygen surface groups (CO + CO₂) corresponds to the carbon activated with phosphoric acid PAC-550.

Fig. 3 shows the FTIR spectrum of the carbon catalysts. Infrared spectroscopy (IR) provides information about the chemical structure of carbon catalysts. All spectra show an absorption band at 3600–3200 cm⁻¹, with a maximum at about 3420 cm⁻¹. This band is characteristic of the stretching O–H vibration of carbon hydroxy compounds, with the broadening of the band indicating an extensive hydrogen bonding and could also be associated to the presence of adsorbed water, although there is not a clear band at 1640 cm⁻¹ to confirm this. This suggests that the analyzed carbons contain hydroxyl groups from carboxyls, phenols or alcohols as previously seen in the TPD analyses. The higher intensity of this band, observed for PAC-550, CaAC-900 and BaAC-700, may result also from the presence of OH corresponding to phosphate, Ca(OH)₂ and Ba(OH)₂

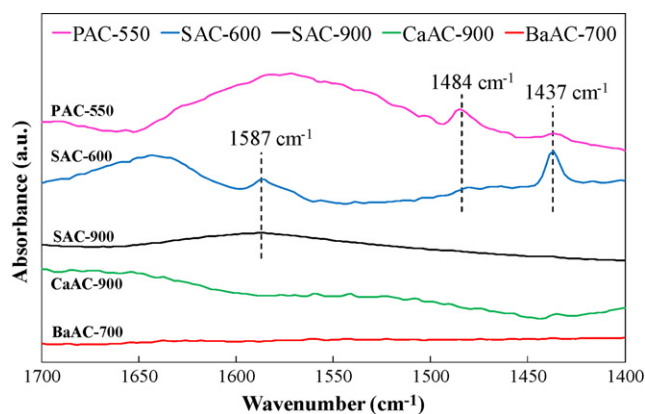


Fig. 4. FTIR spectra resulted from the subtraction of the spectra of the original catalysts from those of the catalysts after adsorption of Py.

surface groups. The presence of aliphatic structures is suggested by the low intensity peaks at around 2950, 2910 and 2840 cm⁻¹. These peaks are due to methyl C–H asymmetric stretch vibration of aliphatic C–H and to the asymmetric/symmetric stretch vibration of methylene C–H, respectively [27]. The spectra of most of the carbons, but BaAC-700, show bands in the range of 1550–1570 cm⁻¹, characteristic of the aromatic ring stretching mode and a wide band between 1300 and 900 cm⁻¹ with the maximum at 1160 cm⁻¹, which is generally attributed to C–O stretching vibrations in acids, alcohols, phenol, ethers, and esters [28,29], although in the case of PAC-550 carbon it could also be associated to the O–C stretching vibrations in the P–O–C (aromatic) linkage [30–32]. In the case of the carbons activated with sulfuric acid, the bands in the 1000–1200 cm⁻¹ range are characteristic of the vibration of the S–O bonds [33]. The broad bands observed at about 1620 and 1440 cm⁻¹ in the IR spectra of CaAC-900 and BaAC-700 can be ascribed to the presence of calcium and barium carbonate surface groups, respectively. The peak at 875 cm⁻¹ corroborates the presence of calcium carbonate groups on the surface of the CaAC-900 carbon.

Chemisorption of basic molecules such as pyridine (Py) is often used to probe the acidity of solids [34–37]. Pyridine interacts with acidic sites because it has a lone electron pair at the nitrogen atom available for donation to a Lewis acidic site and because it can accept a proton from Brønsted sites. Fig. 4 shows the spectra resulted from the subtraction of the spectra of the original catalysts from those of the catalysts after adsorption of Py. Only the carbons obtained by activation with acid precursor, H₃PO₄ and H₂SO₄, show peaks associated to the vibration of adsorbed pyridine. Interaction of pyridine, via the nitrogen lone-pair electrons, with aprotic (Lewis) and protonic (Brønsted) acid sites can be analyzed by following the ring vibration modes 8a and 19b, respectively [38]. The interaction of Py with Lewis type acid sites produces 8a vibration mode usually observed at around 1624 cm⁻¹ and 19b vibration mode at around

Table 3

Mass surface concentration of the carbon catalysts prior and after Py chemisorption at 100 °C obtained by XPS quantitative analysis.

	C (%)	N (%)	O (%)	S (%)	P (%)	Ba (%)	Ca (%)
PAC-550	82.3	0.3	12.9	–	4.5	–	–
SAC-600	83.1	0.5	11.9	4.5	–	–	–
SAC-900	87.0	0.5	7.9	4.6	–	–	–
BaAC-700	69.9	0.5	17.7	–	–	11.9	–
CaAC-900	71.2	0.5	19.2	–	–	–	9.1
PAC-550 (Py)	85.1	0.8	10.0	–	4.1	–	–
SAC-600 (Py)	84.7	0.8	10.5	3.8	–	–	–
SAC-900 (Py)	87.9	0.9	7.0	4.1	–	–	–
BaAC-700 (Py)	70.2	0.8	17.8	–	–	11.2	–
CaAC-900 (Py)	83.1	0.9	11.5	–	–	–	4.5

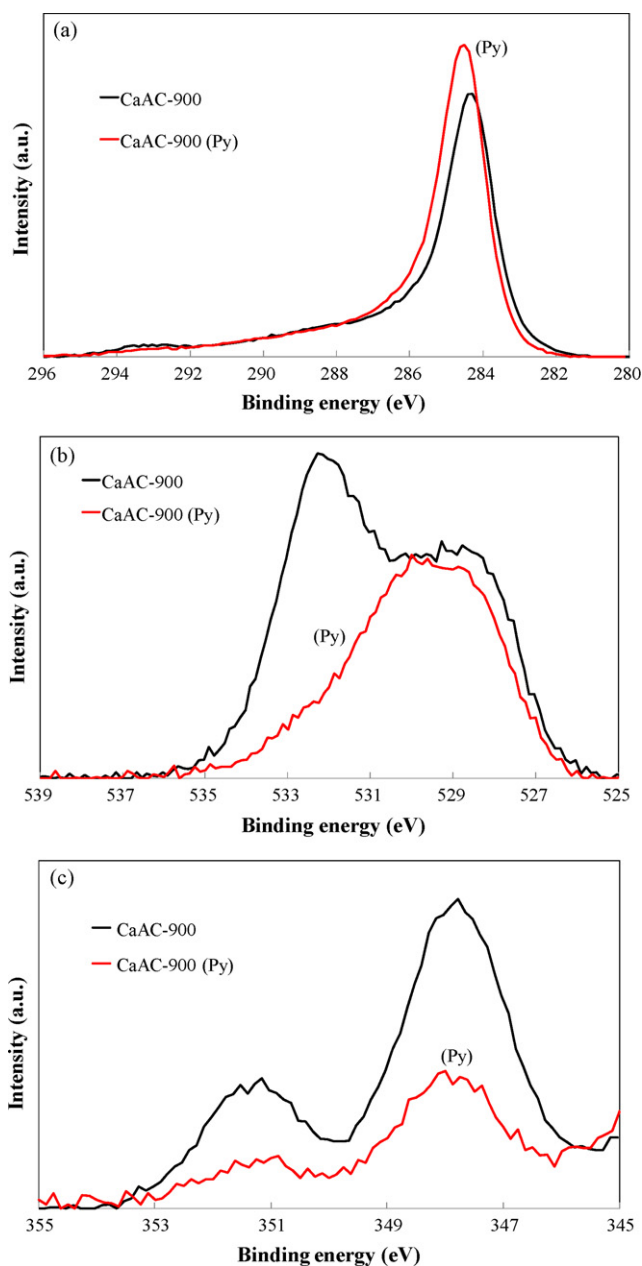


Fig. 5. C(1s) (a), O(1s) (b) and Ca(2p) (c) XPS region spectra for CaAC-900 catalyst before and after Py adsorption.

1452 cm^{-1} . Neither of them is observed in the spectra of SAC-600, SAC-900, CaAC-900 and BaAC-700, suggesting negligible presence of Lewis acid sites on the surface of these carbons. However, the presence of Lewis acid sites seems to be possible on the surface of PAC-550 carbon base on its FTIR spectrum. The pyridine interaction with Brønsted acid sites is observed at 1587 cm^{-1} for 8a vibration mode and at 1437 cm^{-1} for 19b vibration mode. Both peaks are clearly observed in the Py-adsorbed spectra of SAC-600 and PAC-550 carbon, indicating that the acid sites of the carbon surface are predominantly of Brønsted type. The vibration peaks are more clearly observed in the carbon SAC-600 than in the carbon SAC-900, suggesting that the increase in the activation temperature from 600 to $900\text{ }^{\circ}\text{C}$ seems to decrease the surface acidity of the resulting carbon. The band at 1484 cm^{-1} , observed in the PAC-550 and SAC-600 spectra, could be associated to 19a vibration of pyridine ions.

X-ray photoelectron spectroscopy (XPS) analyses were performed to analyze the surface chemical composition of the carbons.

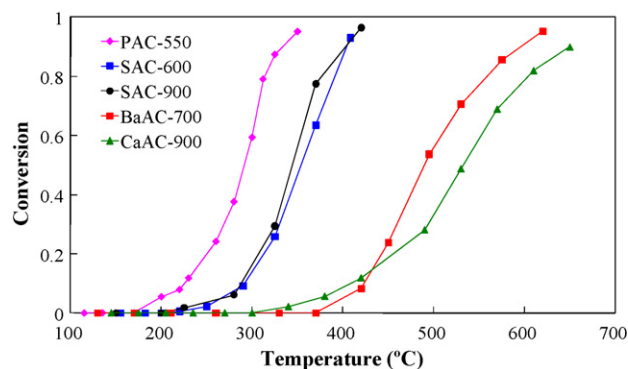


Fig. 6. Steady state conversion of isopropanol on the different carbon based catalysts in the absence of oxygen ($P_{\text{OIPA}} = 0.0185\text{ atm}$, $W/F_{\text{OIPA}} = 0.073\text{ g s } \mu\text{mol}^{-1}$).

Table 3 summarizes the mass surface concentrations of the carbon catalysts prior and after pyridine chemisorption at $100\text{ }^{\circ}\text{C}$. The main elements found on the surfaces of the carbons were carbon and oxygen. Lower amount of phosphorus, sulfur, calcium and barium was retained in the structure during the activation procedure, depending on the activating agent used in the preparation of the carbon, H_3PO_4 , H_2SO_4 , $\text{Ca}(\text{OH})_2$ and $\text{Ba}(\text{OH})_2$, respectively. Nitrogen, usually present in the biomass materials, was also detected, although in a very low concentration. During the activation these elements are retained into the structure of the activated carbons, either combined with the organic structure or physically entrapped. In the case of the activation with sulfuric acid, the increase of the activation temperature (from 600 up to $900\text{ }^{\circ}\text{C}$) results in a lower oxygen atomic surface concentration (observed also in the TPD experiments), due to the removal of the oxygen surface groups at higher temperatures. The differences observed between the oxygen concentration in TPD and XPS analyses indicate a non-homogeneous distribution of the oxygen on the carbon material surface, given that XPS provides information only of the external surface, while TPD analyses provide information of both external and internal surface. Adsorption of Py on PAC-550 results in a slight increase of N and C and in the reduction of O and P, probably due to Py adsorption on the H of the surface phosphate groups, as it was indicated by the FTIR study.

The values of Table 3 for BaAC-700 confirm the absence of adsorption of Py on this basic catalyst. However, an increase of the amount N and C and a significant decrease of Ca and O are observed for CaAC-900 after Py adsorption. This result seems to indicate that this catalyst also presents acid sites. Fig. 5 represents the C(1s) (a), O(1s) (b) and Ca(2p) (c) XPS region spectra for CaAC-900 catalyst. As in the case of the catalysts obtained by acid activation (PAC-550, SAC-600 and SAC-900) the decrease of the signal intensity in the Ca spectrum and that of the O(1s) at 532.0 eV , with an increase of the signal intensity in the C(1s) spectrum suggest that Py is adsorbed on $\text{Ca}^{\delta+}\text{-O}$ site, i.e., calcium with positive electronic density, as a consequence of the formation of substoichiometric surface specie. This specie, which may act as acid surface site, could be formed by decomposition of part of the surface carbonates at the high carbonization temperature ($900\text{ }^{\circ}\text{C}$) used in the preparation of this carbon. The presence of acid sites on the surface of the CaAC-900 catalyst is supported by the production of propylene during the decomposition of isopropanol on this catalyst, as it will be seen later.

Fig. 6 represents the steady state conversion of isopropanol on the different carbon based catalysts in the absence of oxygen ($P_{\text{OIPA}} = 0.0185\text{ atm}$, $W/F_{\text{OIPA}} = 0.073\text{ g s } \mu\text{mol}^{-1}$). As expected, isopropanol conversion increases with the reaction temperature. The acidic carbons PAC-550, SAC-600 and SAC-900 show higher steady state conversions than those corresponding to the basic carbons

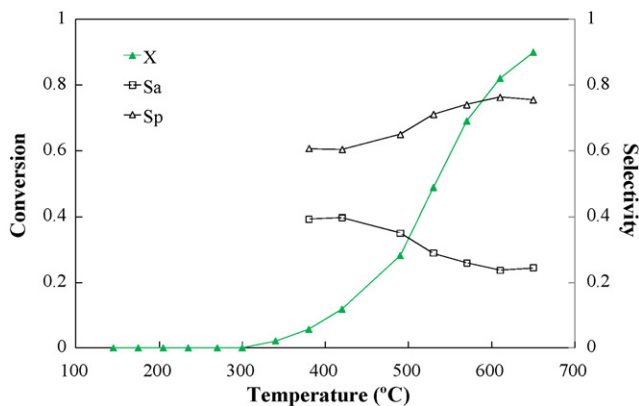


Fig. 7. Steady state conversion of isopropanol (X) and selectivity to acetone (Sa) and propylene (Sp) on CaAC-900 carbon based catalysts in the absence of oxygen ($P_{\text{OIPA}} = 0.0185 \text{ atm}$, $W/F_{\text{OIPA}} = 0.073 \text{ g s } \mu\text{mol}^{-1}$).

BaAC-700 and CaAC-900. The increase of the temperature, from 600 to 900 °C, during the activation of the carbon with sulfuric acid shows very little influence in the isopropanol steady state conversion. The highest conversions were obtained using PAC-550 as catalyst. The activation of lignocellulosic residues with phosphoric acid has proven to yield acid carbon catalysts in a single step with a high activity in the alcohol decomposition [19,39,40]. The –OH groups of phosphates and polyphosphate esters, formed during the activation step, can act as Brønsted acid sites (in agreement with the Py-FTIR analysis), giving up protons (H^+) during the isopropanol dehydration reaction [19].

The differences in the surface chemistry of the carbon catalysts obtained with acidic or basic activating agents are clearly observed analyzing the selectivity of the isopropanol decomposition in a helium flow. In a previous study [19], we have shown that the high activity of different acid carbon catalyst in the isopropanol decomposition is due to their high acidity, as revealed the ammonia TPD, and not by their porous structure development. Table 4 presents the selectivity to propylene (Sp) and acetone (Sa) for the different catalysts at a isopropanol conversion of 0.6, as well as the reaction temperature at which this conversion is reached. In the case of the acidic carbons, PAC-550, SAC-600 and SAC-900, isopropanol decomposition reaction yields only propylene and water as reaction products ($\text{Sp} = 100\%$). This is a consequence of the acidity of the surface of these carbons, since it is well known that isopropanol dehydrates to propylene over solid acid catalysts. On the other hand, Figs. 7 and 8 represent the evolution of isopropanol conversions and selectivities at the steady state as a function of the reaction temperature in a helium flow using CaAC-900 and BaAC-700 as catalysts ($P_{\text{OIPA}} = 0.0185 \text{ atm}$, $W/F_{\text{OIPA}} = 0.073 \text{ g s } \mu\text{mol}^{-1}$). In the case of these carbons, besides to propylene as dehydration product, acetone is also obtained as isopropanol dehydrogenation product. For BaAC-700 catalyst the selectivity to acetone is always higher than 80% for the steady state conversion studied, as expected

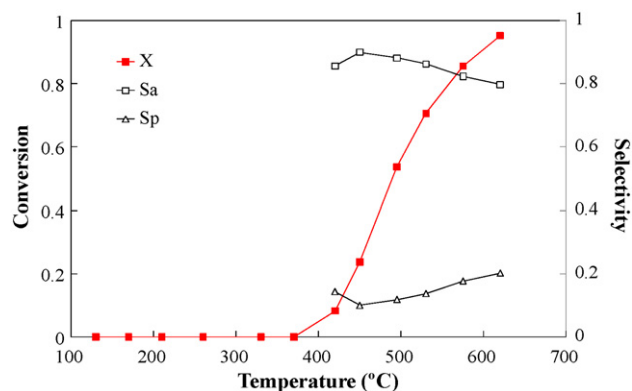


Fig. 8. Steady state conversion of isopropanol (X) and selectivity to acetone (Sa) and propylene (Sp) on BaAC-700 carbon based catalysts in the absence of oxygen ($P_{\text{OIPA}} = 0.0185 \text{ atm}$, $W/F_{\text{OIPA}} = 0.073 \text{ g s } \mu\text{mol}^{-1}$).

for a catalyst with a basic surface. In the case of CaAC-900 catalyst, a selectivity to about 40% for acetone is observed at low reaction temperatures and conversions. An increase of the reaction temperature increases both the conversion and propylene selectivity. The formation of acetone, through the dehydrogenation of isopropanol, takes place on the basic sites of these two catalysts. The relatively high production of propylene on the CaAC-900 is due to the presence of surface acid sites, as evidenced by the IR results.

The influence of the presence of oxygen in the inlet stream (21 vol.%) has been analyzed. In the case of the basic carbon catalysts, CaAC-900 and BaAC-700, these carbons begin to burn out at a significant rate at temperatures of around 300 °C, before isopropanol begins to react. Figs. 9 and 10 represent the evolution of isopropanol steady state conversions and selectivities as a function of the reaction temperature in air flow (21% O_2) using PAC-550 and SAC-900 as catalysts ($P_{\text{OIPA}} = 0.0185 \text{ atm}$,

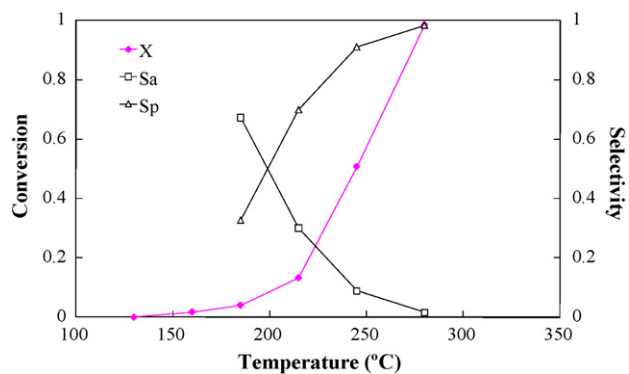


Fig. 9. Steady state conversion of isopropanol (X) and selectivity to acetone (Sa) and propylene (Sp) on PAC-550 carbon based catalysts in the presence of oxygen ($P_{\text{OIPA}} = 0.0185 \text{ atm}$, $W/F_{\text{OIPA}} = 0.073 \text{ g s } \mu\text{mol}^{-1}$).

Table 4
Selectivity to propylene (Sp) and acetone (Sa) and reaction temperature for the different catalysts at a isopropanol conversion of 0.6.

Sample	Gas	Sp (%)	Sa (%)	$T_{X=0.6}$ (°C)
PAC-550	He	100	0	300
SAC-600	He	100	0	365
SAC-900	He	100	0	354
BaAC-700	He	13	87	505
CaAC-900	He	73	27	556
PAC-550	Air	92	8	255
SAC-900	Air	90	10	258
BaAC-700	Air	–	–	Burn out
CaAC-900	Air	–	–	Burn out

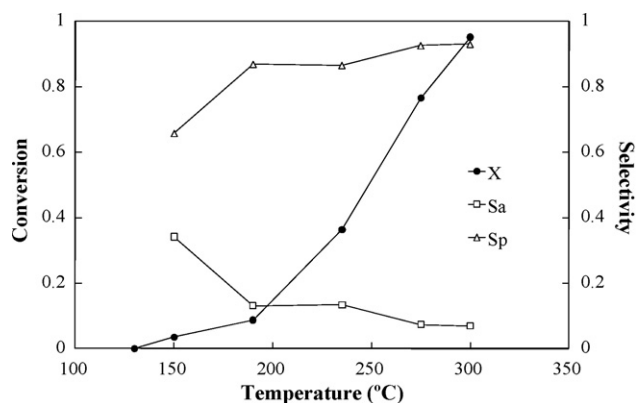


Fig. 10. Steady state conversion of isopropanol (X) and selectivity to acetone (Sa) and propylene (Sp) on SAC-900 carbon based catalysts in the presence of oxygen ($P_{\text{OIPA}} = 0.0185$ atm, $W/F_{\text{OIPA}} = 0.073$ g s μmol^{-1}).

$W/F_{\text{OIPA}} = 0.073$ g s μmol^{-1}). The presence of oxygen produces a higher reaction rate and a change in the product distribution for the acid catalysts PAC-550 and SAC-900 (see Figs. 9 and 10 and Table 4). Furthermore, in the presence of oxygen, acid carbon catalysts produce acetone by oxidative dehydrogenation of isopropanol and propylene by dehydration of the alcohol.

These results are in agreement with the previously reported by Grunewald and Drago [41] who studied the conversion reactions of ethanol catalyzed by carbon. In the absence of oxygen, ethanol transformation was catalyzed at 230 °C mainly to ethylene. However, in the presence of oxygen, acetaldehyde and ethyl acetate were the major products. These authors indicated that the carbon surface active sites were reduced by ethanol and regenerated by the oxygen. In a similar sense, Carrasco-Marin et al. [42] stated that when using surface-treated activated carbons as catalysts for the decomposition of ethanol, the presence of air in the reactant mixture cleaned some of carbon surface sites, increasing the dehydrogenation activity and decreasing the dehydration one.

It can be assumed that isopropanol decomposition reaction follows a global first-order kinetics described by the following equation in the absence of diffusional effects:

$$\ln\left(\frac{1}{1-X}\right) = k \cdot P_{\text{OIPA}} \cdot \frac{W}{F_{\text{OIPA}}}$$

where k is the apparent rate constant, W is the catalyst weight, F_{OIPA} is the reactant molar flow rate, P_{OIPA} is the reactant partial pressure and X is the conversion. The activation energy is derived from the Arrhenius equation. Table 5 summarizes the values of the kinetic parameters (k_0 is the preexponential factor and E_a is the activation energy) for all the catalysts, obtained from the Arrhenius plots represented in Fig. 11. Values from 63 to 88 kJ/mol have been obtained, which are in the same range than those previously obtained for carbon based acid catalysts prepared from biomass by phosphoric acid activation for the dehydration of isopropanol [19]. It seems that the nature and amount of acid/basic sites affect the catalytic activity and the product distribution for the isopropanol

Table 5
Apparent kinetic parameters for isopropanol conversion.

Sample	Gas	E_a (kJ/mol)	$\ln k_0$
PAC-550	He	75	19.6
SAC-600	He	77	20.3
SAC-900	He	70	16.9
CaAC-900	He	70	13.8
BaAC-700	He	88	15.0
PAC-550	Air	86	23.8
SAC-900	Air	63	18.0

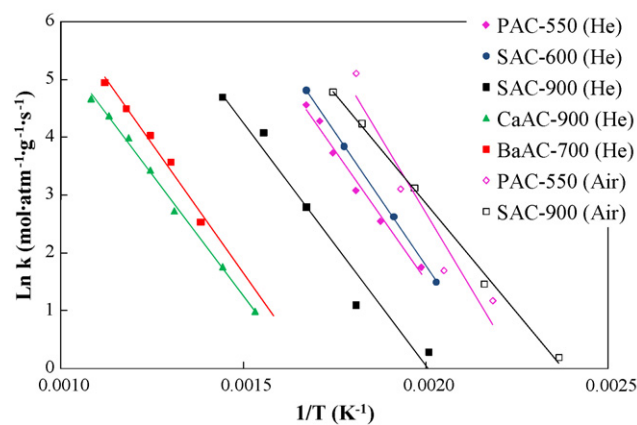


Fig. 11. Arrhenius plots for isopropanol decomposition using air and helium as reaction gas.

decomposition reaction. The literature shows a broad spectrum of activation energy values for this reaction, ranging from 12 to 133 kJ/mol [18,43,44]. This large variation in the activation energy values could be due to the different type of interaction between isopropanol molecules and the catalyst surface active sites. Also diffusional limitations due to different experimental conditions may reduce the value of the apparent activation energy.

4. Conclusions

Chemical activation of biomass waste with different activating agents allows the preparation of activated carbons with a relatively highly porous development and different surface chemistry properties. Acidic and basic carbon based catalysts have been prepared by chemical activation of olive stone waste with H_3PO_4 and H_2SO_4 of acid character and $\text{Ca}(\text{OH})_2$ and $\text{Ba}(\text{OH})_2$ of basic character. In the absence of oxygen acidic carbon catalysts dehydrate isopropanol to propylene with 100% of selectivity. In the case of the basic carbon catalysts, BaAC-700 mainly dehydrogenate isopropanol to acetone, with low production of propylene. CaAC-900 carbon presents acid and basic surface sites and propylene and acetone are obtained on this catalyst. The presence of oxygen produces a higher reaction rate and a change in the product distribution for the acid catalysts PAC-550 and SAC-900. Furthermore, in the presence of oxygen, acid carbon catalysts produce acetone by oxidative dehydrogenation of isopropanol and propylene by dehydration of the alcohol.

Acknowledgements

We gratefully acknowledge to the Spanish DGICYT, Projects CTQ2006-11322 and CTQ2009-14262.

References

- [1] C. Branca, P. Giudicianni, C. Di Blasi, *Ind. Eng. Chem. Res.* 43 (2003) 3190.
- [2] A.E. Pütün, A. Özcan, H.F. Gerçel, E. Pütün, *Fuel* 8 (2001) 1371.
- [3] J.D. Adjaye, S.P.R. Katikaneni, N.N. Bakhshi, *Fuel Process. Technol.* 48 (1996) 115.
- [4] A.G. Gayubo, A.T. Aguayo, A. Atutxa, R. Aguado, J. Bilbao, *Ind. Eng. Chem. Res.* 43 (2004) 2610.
- [5] A.G. Gayubo, A.T. Aguayo, A. Atutxa, R. Aguado, M. Olazar, J. Bilbao, *Ind. Eng. Chem. Res.* 43 (2004) 2619.
- [6] H. Koempel, W. Liebner, *Stud. Surf. Sci. Catal.* 167 (2007) 261–267.
- [7] L.R. Radovic, F. Rodríguez-Reinoso, in: P.A. Thrower (Ed.), *Chemistry and Physics of Carbon*, vol. 25, Marcel Dekker, New York, 1997, pp. 243–358.
- [8] R.W. Coughlin, *Ind. Eng. Chem. Prod. Res. Dev.* 8 (1964) 23.
- [9] F. Rodríguez-Reinoso, M. Molina-Sabio, *Carbon* 30 (1992) 1111.
- [10] O. Ioannidou, A. Zabaniotou, *Renewable Sustainable Energy Rev.* 11 (2007) 1966.
- [11] N. Tancredi, T. Cordero, J. Rodríguez-Mirasol, J.J. Rodríguez, *Fuel* 75 (1996) 1701.
- [12] J. Rodríguez-Mirasol, T. Cordero, J.J. Rodríguez, *Carbon* 31 (1993) 87.

- [13] F. Marquez-Montesinos, T. Cordero, J. Rodríguez-Mirasol, J.J. Rodríguez, *Fuel* 81 (2002) 423.
- [14] J.M. Rosas, J. Bedia, J. Rodríguez-Mirasol, T. Cordero, *Fuel* 88 (2009) 19.
- [15] J.M. Rosas, J. Bedia, J. Rodríguez-Mirasol, T. Cordero, *Ind. Eng. Chem. Res.* 47 (2008) 1288.
- [16] C.A. Leon y Leon, L.R. Radovic, in: P.A. Throver (Ed.), *Chemistry and Physics of Carbon*, vol. 25, Marcel Dekker, New York, 1992, pp. 213–310.
- [17] G.S. Szymański, G. Rychlicki, *Carbon* 31 (1993) 247.
- [18] J.M. Campelo, A. Garcia, J.F. Herencia, D. Luna, J.M. Marinas, A.A. Romero, *J. Catal.* 151 (1995) 307.
- [19] J. Bedia, J.M. Rosas, J. Márquez, J. Rodríguez-Mirasol, T. Cordero, *Carbon* 47 (2009) 286.
- [20] S. Brunauer, P.H. Emmett, E. Teller, *J. Am. Chem. Soc.* 60 (1938) 309.
- [21] B.C. Lippens, J.H. de Boer, *J. Catal.* 4 (1965) 319.
- [22] M. Jagtoyen, F. Derbyshire, *Carbon* 36 (1998) 1085.
- [23] R.C. Bansal, J.B. Donnet, F. Stoeckli, *Active Carbon*, Marcel Dekker, New York, 1988 (Chapter 2).
- [24] X. Wu, L.R. Radovic, *Carbon* 44 (2006) 141.
- [25] P.J. Hall, J.M. Calo, *Energy Fuels* 3 (1989) 370.
- [26] F. Kapteijn, G. Abbel, J.A. Moulijn, *Fuel* 63 (1984) 1036.
- [27] A.M. Puziy, O.I. Poddubnaya, A. Martínez-Alonso, F. Suárez-García, J.M.D. Tascón, *Carbon* 43 (2005) 2857.
- [28] J. Zawadzki, in: P.A. Throver (Ed.), *Infrared Spectroscopy in Surface Chemistry of Carbons*, Marcel Dekker, New York, 1989, pp. 147–386.
- [29] P. Vinke, M. van der Eijk, M. Verbree, A.F. Voskamp, H. van Bekkum, *Carbon* 32 (1994) 675.
- [30] L.J. Bellamy, *The Infrared Spectra of Complex Molecules*, Wiley, New York, 1954.
- [31] D.E.C. Corbridge, *J. Appl. Chem.* 6 (1956) 456.
- [32] G. Socrates, *Infrared Characteristic Group Frequencies*, Wiley, New York, 1994.
- [33] M. Waqif, J. Bachelier, O. Saur, J.-C. Lavalley, *J. Mol. Catal.* 72 (1992) 127.
- [34] F.M. Bautista, J.M. Campelo, A. Garcia, D. Luna, J.M. Marinas, A.A. Romero, M.R. Urbano, *J. Catal.* 172 (1997) 103.
- [35] H.A. Benesi, *J. Catal.* 28 (1973) 176.
- [36] H. Knözinger, H. Krietenbrink, P. Ratnasamy, *J. Catal.* 48 (1977) 436.
- [37] A. Corma, C. Rodellas, V. Fornes, *J. Catal.* 88 (1984) 374.
- [38] G. Turnes Palomino, J.J. Cuart Pascual, M. Rodríguez Delgado, J. Bernardo Parra, C. Otero Areán, *Mater. Chem. Phys.* 85 (2004) 145.
- [39] J. Bedia, R. Ruiz-Rosas, J. Rodríguez-Mirasol, T. Cordero, *AIChE J.* 271 (2010) 33.
- [40] J. Bedia, R. Ruiz-Rosas, J. Rodríguez-Mirasol, T. Cordero, *J. Catal.* 271 (2010) 33.
- [41] G.C. Grunewald, R.S. Drago, *J. Am. Chem. Soc.* 113 (1991) 1636.
- [42] F. Carrasco-Marín, A. Mueden, C. Moreno-Castilla, *J. Phys. Chem. B* 102 (1998) 9239.
- [43] W. Turek, J. Haber, A. Krowiak, *Appl. Surf. Sci.* 252 (2005) 823.
- [44] P. Trens, V. Stathopoulos, M.J. Hudson, P. Pomonis, *Appl. Catal. A: Gen.* 263 (2004) 103.